
ELSEVIER

Nuclear Instruments and Methods in Physics Research B 164–165 (2000) 203–211

NIM B
Beam Interactions with Materials & Atoms

www.elsevier.nl/locate/nimb

Impact-parameter dependent energy loss of screened ions

G. dze M. Azevedo [a], P.L. Grande [a,*], G. Schiwietz [b]

[a] *Instituto de Física da Universidade Federal do Rio Grande do Sul, Avenida Benito Goncalvez 9500, 91501-970, Porto Alegre, Brazil*
[b] *Bereich F, Hahn-Meitner-Institut Berlin, Glienicker Str. 100, D-14109, Berlin, Germany*

Abstract

We describe a simple model for the electronic energy loss as a function of the impact parameter for screened projectiles at high velocities. The physical inputs are the projectile screening potential, the electronic density and the oscillators strengths for the target electrons. An excellent agreement with full first-order Born calculations is obtained. The results are then used to compute the angular dependence of the electronic energy loss under channeling conditions.

PACS: 34.50. Fa

1. Introduction

At very high projectile speeds the electronic energy loss is dominated by ionization and excitation processes and it is very well described by first-order perturbation theory. By decreasing the ion energy higher-order effects come into play. They become very important at energies where charge-changing processes are also likely to occur. Thus, a clear separation of these processes turns out to be a complicated task even for light projectiles from the theoretical as well as from the experimental point of view. In order to describe the energy loss properly, the contribution due to projectiles carrying bound electrons must be considered. The problem of the stopping power of screened projectiles was first studied by Dalgarno and Griffing [1] in the plane-wave Born approximation (PWBA) for the most simple collision system (H on H) in the mid 1950s and has been extended for other atomic collisional systems using the Bethe theory [2–4]. More recently, Sigmund [5] has developed a model for the charge-dependent electronic stopping of swift heavy ions in the framework of Bohr's classical theory and Bethe–Bloch stopping theory. For solids, the first attempt to include the influence of bound projectile electrons on the stopping power was performed by Ferrell and Ritchie [6] in the dielectric-function formalism. Later many other investigations were performed [7–11] introducing the effective-charge concept. Nowadays the most elaborate method to include the projectile screening at low velocities is through the density functional theory by Echenique and coworkers [12].

The effect of the electronic screening is not only important for the total electronic stopping power but also for the impact parameter dependent

* Corresponding author.
E-mail address: grande@if.ufrgs.br (P.L. Grande).

0168-583X/00/$ - see front matter
PII: S0168-583X(99)01074-5

energy loss. This differential information is crucial for the understanding and analysis of channeling experiments [13–16] as well as for the interpretation of the angular dependences of energy losses in ion-transmission measurements through thin foils [17].

The impact parameter dependent energy loss of screened projectiles at high velocities can be calculated in first-order Born approximation for the electronic motion where the projectile moves according to classical mechanics, the so-called semi classical approximation (SCA). The first full SCA calculations for the electronic energy loss of bare ions (here full means that the sum over all final states is performed explicitly) were performed by Kabachnik et al. [18] and later by Schiwietz and Grande [1] and by Moneta and Czerbniak [19]. These calculations have been further extended to include screening effects in [20,21]. A few years later appeared the first coupled-channel calculations [22] which were also extended to screened Coulomb interactions. Since these improved calculations have become available only very recently, the computer simulation community has used semi-empirical formulas [23] or other strongly simplified models [24–26] in order to deal with inelastic collisions.

For the simulation of ion transport in matter even an SCA calculation for the excitation and ionization processes is too extensive to be included in the computer codes. Therefore, simple methods are required to predict absolute electronic energy losses in a reliable way without using large scale calculations. Here we describe an extension of the perturbative convolution approximation (PCA), which yields remarkable agreement with full SCA results for bare ions [27]. The extended model accounts additionally for the electronic energy loss of *screened* ions at high velocities and for all impact parameters. The projectile electrons are treated as a frozen charge density and thus, they only screen the Coulomb interaction of the projectile nucleus. The physical inputs of the present model are only the electronic screening function of the projectile, the electronic density and the oscillator strengths for each optically allowed transition of the target electrons. If not indicated, otherwise atomic units ($e = 1, m = 1, \hbar = 1$) will be used throughout the paper.

2. PCA model for screened projectiles

A detailed description of the perturbative convolution model (PCA) for bare ions may be found elsewhere [27,28]. Here we present only a short outline of the method. The electronic energy loss is calculated from the expression

$$Q(b) = \sum_f |a_f(\vec{b})|^2(\epsilon_f - \epsilon_0), \tag{1}$$

which involves a sum over all final target states with energies ϵ_f and the corresponding computation of transition amplitudes a_f for each impact parameter. Usually this demands an computational effort that precludes the use of Eq. (1) in a computer simulation code. Therefore we search for an approximate solution without the necessity of performing a large-scale calculation.

In a recent work [27] we have proposed a simple formula for $Q(b)$ (called PCA) that reproduces virtually SCA results for all impact parameters for bare projectiles. An extension of this model for projectiles carrying bound electrons will be described here by considering three types of screened Coulomb potentials for the interaction between the projectile ion and the target electrons. These potentials contain not only the Coulomb part due to the projectile-nuclear charge but also the static potential produced by the projectile electrons that screen the projectile-nuclear charge. Such a potential can be calculated from

$$V(\vec{R} - \vec{r}) = -\frac{Z_\mathrm{p}}{|\vec{R} - \vec{r}(t)|} + \sum_n^{n_\mathrm{p}} \int d^3r' \frac{|\Phi_n(\vec{r}')|^2}{|\vec{R} - \vec{r} - \vec{r}'|}, \tag{2}$$

where Z_p is the projectile nuclear charge, Φ_n are the projectile-electron wave functions and n_p is the

[1] The numerical procedures are the same as used for coupled channel calculations in [22,42–44].

number of projectile electrons. The wave functions Φ_n for each electron n of the projectile can be obtained according to the Hartree–Fock–Slater procedure [29]. In this formulation we neglect dynamic screening (a time dependence of Φ_n due to projectile polarization, excitation and/or ionization), Pauli correlation (antisymmetrization of the projectile and target centered wave functions), and dynamic correlation effects due to the residual electron–electron interaction. Here the projectile electrons just screen the projectile nucleus (screened-Coulomb contribution), i.e., the projectile electrons remain in the ground-state when the target is excited. Thus, we also neglect the so-called antiscreening effect, where the electron–electron interaction between the bound projectile electrons and the target electrons results in an enhancement of the ionization and excitation cross sections at intermediate to high energies [30–32].

Here we have considered three types of projectile screening potentials:

1. The Bohr-like screening potential

$$V(\vec{r}-\vec{R}) = -Z_{\mathrm{p}}\frac{\mathrm{e}^{-\alpha|\vec{r}-\vec{R}|}}{|\vec{r}-\vec{R}|},$$

is the electrostatic potential produced by a foreign point charge Z_{p} placed in a homogeneous electron gas. Therefore, the Bohr-like potential roughly describes the polarization of the valence electrons in a solid due to the presence of the projectile. For slow ions, the parameter α can thus be determined from the Debye screening length [33].

2. The single-zeta screening potential,

$$V(\vec{r}-\vec{R}) = -\left(\frac{(Z_{\mathrm{p}}-n_{\mathrm{p}})}{|\vec{r}-\vec{R}|} + n_{\mathrm{p}}\frac{\mathrm{e}^{-\alpha|\vec{r}-\vec{R}|}}{|\vec{r}-\vec{R}|} \times \left(1+\frac{\alpha}{2}|\vec{r}-\vec{R}|\right)\right),$$

describes the interaction of the active target electron with projectiles carrying one or two electrons ($n_{\mathrm{p}} = 1, 2$) in hydrogen-like 1s orbitals. In this case the parameter α is obtained from an effective projectile charge $Z_{\mathrm{p}}^{\mathrm{eff}}$ (as $\alpha = 2Z_{\mathrm{p}}^{\mathrm{eff}}$).

3. The general screening potential,

$$V(\vec{r}-\vec{R}) = -\left(\frac{(Z_{\mathrm{p}}-n_{\mathrm{p}})}{|\vec{r}-\vec{R}|} + n_{\mathrm{p}}\sum_{i}^{n_{\max}}\frac{\mathrm{e}^{-c_i|\vec{r}-\vec{R}|}}{|\vec{r}-\vec{R}|} \times (a_i + b_i|\vec{r}-\vec{R}|)\right),$$

is a sum of generalized single zeta-potentials and it is appropriate for projectiles carrying many bound electrons. The coefficients a_i, b_i and c_i are obtained by a fit to the numerically determined potential from Eq. (2). Usually, the number of single-zeta potential terms, $n_{\max}$, corresponds to the number of atomic shells of the projectile.

As in [27,28] and in what follows, we will describe the limiting behavior of $Q(b)$ at small and large impact parameters, in order to extract a common expression for the energy transfer that interpolates between the asymptotic solutions.

At *large impact parameters* the so-called dipole approximation for $V(\vec{r}-\vec{R}(t))$ is used, where

$$V(\vec{r}-\vec{R}(t)) \approx V(\vec{r}-\vec{R}(t))_{|_{\vec{r}=0}} + \vec{r}\cdot\vec{\nabla}_{\vec{r}}V(\vec{r}-\vec{R}(t))_{|_{\vec{r}=0}} \tag{3}$$

and thus, an analytical expression [34,35] for $Q(b)$ may be obtained in the form

$$Q(b) = \frac{1}{2}\sum_i f_i|\hat{E}(b,\omega_i)|^2 \tag{4}$$

$$= T(b)\sum_i f_i g_{\mathrm{screen}}\left(\frac{\omega_i b}{v_{\mathrm{p}}}\right), \tag{5}$$

with $\hat{E}(b,\omega)$ being the Fourier transform of the projectile electrical field ($\vec{E}(t) = -\nabla_{\vec{r}}V(\vec{r}-\vec{R}(t))_{|_{\vec{r}=0}}$) and $T(b) = 2Z^2/v_{\mathrm{p}}^2b^2$ is the energy transfer of an unscreened projectile to an electron at rest in the framework of classical impulse approximation.

Inserting the Bohr-like screening potential into Eq. (4) the function g_{screen} reads

$$g_{\mathrm{screen}}(b) = ((\omega b/v_{\mathrm{p}})^2 + (\alpha b)^2)K_1^2\left(\sqrt{(\omega b/v_{\mathrm{p}})^2 + (\alpha b)^2}\right) + (\omega b/v_{\mathrm{p}})^2K_0^2\left(\sqrt{(\omega b/v_{\mathrm{p}})^2 + (\alpha b)^2}\right).$$

A similar expression was also found in [5]. For the other screening potentials (single-zeta and

general), the functions g_{screen} are presented in Appendix A.

In the equations above, K_0 and K_1 are the modified Bessel functions, ω_i are the transition energies ($\omega_i \equiv \epsilon_i - \epsilon_0$), f_i are the well known dipole-oscillator strengths ($f_i = 2\,|\langle i|z|0\rangle|^2\,(\epsilon_i - \epsilon_0)$), which fulfill the sum rule $\sum_i f_i = 1$ [36] and v_{p} is the projectile speed. The function $g_{\text{screen}}(x;\gamma)$ for the Bohr-like potential is presented as dashed and dotted line in Fig. 1, where

$$x = \sqrt{(\omega b/v_{\text{p}})^2 + (\alpha b)^2}$$

and

$$\gamma = \frac{\alpha^2}{(\omega/v_{\text{p}})^2 + \alpha^2}.$$

In Fig. 1 the two limiting cases of the function $g_{\text{screen}}(x;\gamma)$ are displayed: $\gamma = 1$ for strong screening and $\gamma = 0$ for the bare Coulomb case. The solutions given above (and in the Appendix A) are exact for asymptotically large values of b, but are completely inadequate for small impact parameters, where other multipole terms gain importance. In fact, they diverge for $b \to 0$ since $\sum_i f_i g_{\text{screen}}(\omega_i b/v_{\text{p}}) = 1$ and $Q(b)$ turns out to be equal to the classical energy transfer from the *unscreened* projectile to an electron at rest.

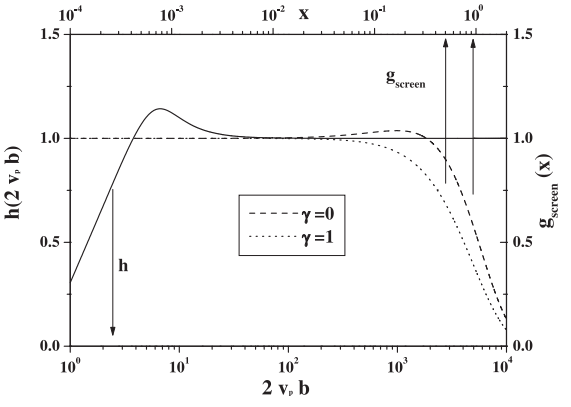

Fig. 1. The functions g_{screen} for the Bohr-like potential and h from Eq. (8) are plotted versus the corresponding scaled impact parameters. At high ion velocities the flat parts of both functions have a considerable overlap.

For *intermediate impact parameters* b (somewhat larger than the shell radius, r_{shell}) and at high velocities a closure approximation can be used in Eq. (1) (after neglecting an exponential factor in the first-order amplitude). This procedure results in an expression identical to the classical energy transfer to an electron at rest, whose time-dependent motion during the collision is neglected. Thus, the behavior of $Q(b)$ for intermediate impact parameters can be directly obtained from those for large impact parameters by simply setting $\omega_i = 0$ in the equations above. For small impact parameters both the large and intermediate impact-parameter approximation yield $Q(b) = T(b)$. At small impact parameters, however, maximum energy transfers as high as $\omega_i = 2v_{\text{p}}^2$ gain importance and a proper treatment of the two-body collision kinematics becomes necessary.

For *small impact parameters* the active target electron interacts mainly with the bare projectile nucleus. For this reason screening effects may be neglected in this range of impact parameters. For bare ions at high projectile velocities, the energies of ejected electrons are large compared to their binding energy. In this case, the influence of the target potential can also be neglected and correspondingly the final target continuum states are replaced by plane waves. As we have shown recently [27], an analytical formula for $Q(b)$ can be derived by use of the peaking approximation. The resulting energy loss reads

$$Q(b) = \int \mathrm{d}^2 r_T\, \mathscr{T}(\vec{b} - \vec{r}_T) \int \mathrm{d}z\, \rho(\vec{r}_T, z), \tag{6}$$

with

$$\mathscr{T}(b) = \frac{2Z^2}{v_{\text{p}}^2 b^2} h(2v_{\text{p}}b) = T(b)h(2v_{\text{p}}b) \tag{7}$$

and

$$h(x) = \frac{x^2}{2}\int_0^1 \mathrm{d}y\, y K_0(xy^2) J_0\left(xy\sqrt{1-y^2}\right) \approx \frac{x^2}{x^2+\beta_1^2} + \frac{\beta_2 x^2}{1+\beta_3 x^4}, \tag{8}$$

with $\beta_1 = 1.551$, $\beta_2 = 0.0123$, $\beta_3 = 0.0009$. A similar expression was also derived in [37] but

involving Bessel functions of higher order. As it can be seen in Fig. 1, the function $h(2v_p b)$ approaches zero for $b \ll 1/v_p$ and it reaches 1 for large values of b. In the latter case, the energy transfer resembles again the classical energy transfer to a statistical distribution of electrons at rest. It is pointed out that the results from Eq. (7) are target independent.

In the following we extend our simple formula for bare projectiles [27,28] to screened ones using the same type of product ansatz,

$$Q(b) = \int \mathrm{d}^2 r_T \, \mathscr{K}(\vec{b} - \vec{r}_T) \int \mathrm{d}z \, \rho(\vec{r}_T, z), \tag{9}$$

with

$$\mathscr{K}(b) = \frac{2Z^2}{v_p^2 b^2} h(2v_p b) \sum_i f_i \, g_{\mathrm{screen}}\left(\frac{\omega_i b}{v_p}\right). \tag{10}$$

This function $\mathscr{K}$ joins smoothly all regions of impact parameters described above. The first two terms in Eq. (10) describe violent binary collisions and the last term accounts for the screening effect by strongly reducing the long ranged dipole transitions. The first integral $\int \mathrm{d}^2 r_T \ldots$ in Eq. (9) describes a convolution with the initial electron density also outside the projectile path and yields non-local contributions to the energy loss. It is noted that these non-local contributions are neglected in most previous simple energy loss models. In what follows, we will use the abbreviation PCA (perturbative convolution approximation) for the results calculated according to Eqs. (9) and (10).

3. Results and discussion

In Fig. 2 we show the results of the present model for the mean energy loss (due to target contribution) of H atoms colliding with H atoms (curves) at 500 keV/u. These results are compared with full first-order SCA calculations (symbols) for three different potentials: Coulomb potential, Bohr-like potential (with $\alpha = 2$) and single-zeta potential (with $Z_p^{\mathrm{eff}} = 1$). The electronic densities were obtained from the analytical formula for the H target. The oscillator strengths are taken from

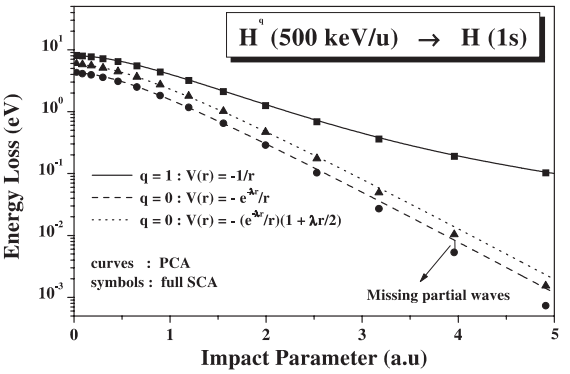

Fig. 2. Energy-loss results of the PCA model (lines) compared with SCA calculations for three different potentials: pure Coulomb potential, Bohr-like potential (with $\alpha = 2$) and single-zeta potential (with $Z_p^{\mathrm{eff}} = 1$). These parameters correspond to collisions of neutral H projectiles with free H atoms.

[38] for H. As Fig. 2 shows, the agreement of the PCA with the SCA calculations is very good for a large range of impact parameters. Nevertheless, at first sight, it may be seen that the agreement for $b > 2.5$ a.u. is better for the pure Coulomb potential than for the screened ones. Indeed, the apparent disagreement for the screened cases is attributed to the truncation of the basis (partial waves up to $l = 17$) in which the wave functions are expanded in the SCA calculations. As we have checked, the more partial waves are included in the SCA calculations the better is the agreement with PCA-screening calculations at large impact parameters.

The results of the present model are shown in Fig. 3 for a system of interest for ion beam analysis, namely He on Si. Calculations are performed for Si atoms exciting He^+ ions at 500 keV/u (corresponding to the electron-loss processes and projectile excitation). The suitable potential for this situation is the general screening potential, as described above. Here, the electronic densities were obtained from Hartree–Fock–Slater densities for Si [29]. As can be observed, the agreement of PCA with SCA (using the same projectile screening function) calculations is very good. Concerning the impact parameter range $b > 2.5$ a.u., the apparent differences are again attributed to missing partial waves in the SCA calculations.

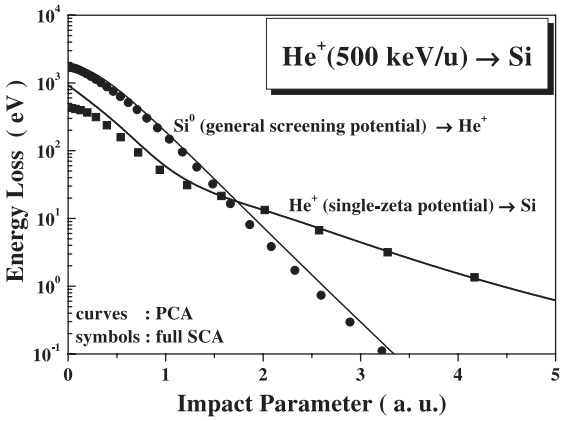

Fig. 3. Comparison of the results of the PCA and the SCA (using partial wave up to $l = 17$) for a He^+ ion colliding with a Si atom. At large impact parameters the flatter curve describes the energy loss due to excitation/ionization of the Si target. The steeper curve is the energy loss due to the ionization and excitation of the projectile during the collision process.

Fig. 3 also displays the result of energy-loss calculations for Si excitation/ionization by He^+ projectiles. Here, the appropriate screening potential is the single-zeta potential (with $Z_p^{\text{eff}} = 2$). For the target parameters the electronic density for each sub-shell was taken into account. For each sub-shell, however, only a single oscillator strength and a mean transition energy was considered according to the analysis performed in [27]. The mean transfer energy $\overline{\omega}_s$ was assumed to be equal to vI_s with I_s being the binding energy of the shell s under consideration and

$$v = I_{\text{Bethe}} \Big/ \exp\left(\frac{1}{N}\sum_s n_s \ln\left(I_s\right)\right), \tag{11}$$

where n_s is the number of electrons of the shell s and N is the total number of electrons. For Si the Hartree–Fock–Slater [29] values of I_s were used ($I_{1s} = 1823$ eV, $I_{2s} = 151$ eV, $I_{2p} = 108$ eV, $I_{3s} = 13.57$ eV, $I_{2p} = 6.54$ eV). This choice is consistent with the mean energy transfer I_{Bethe} from the Bethe formula. Here we have used $I_{\text{Bethe}} = 173$ eV for solid Si. It is pointed out that this value differs considerably from the free-atom one [39].

The agreement of PCA with SCA is very good for large impact parameters. However, for small impact parameters ($b \ll 1$) significant deviations are found. The reason is an overestimated inner-shell contribution that was previously also found for bare projectiles on Ne atoms [27]. It shows the limitation of the present model which is valid only for projectile speeds exceeding the mean orbital electron velocity.

In Fig. 4 we present the experimental data [40] on the electronic energy loss for 500 keV/u He ions channeled in Si $\langle 1\,0\,0\rangle$ as a function of the tilt angle Ψ of the beam relative to the channeling axis. The variation of the electronic energy loss with the angle Ψ reflects the impact-parameter dependence of the mean energy transfer $Q(b)$ in single collisions. The mean energy lost by the projectile after penetrating a depth z in the Si crystal is given by

$$\Delta E(\Psi) = \frac{\int_A \mathrm{d}^2\rho \int_0^z \mathrm{d}x\, Q(\vec{\rho})\Phi(\Psi,\vec{\rho},x)}{d\int_A \mathrm{d}^2\rho \int_0^z \mathrm{d}x\, \Phi(\Psi,\vec{\rho},x)}, \tag{12}$$

where A is the transversal area of the Si $\langle 1\,0\,0\rangle$ channel, $\vec{\rho}$ is the position relative to the center of the channel, $\Phi(\Psi,\vec{\rho},x)$ is the ion flux distribution at the distance $\vec{\rho}$ and depth x, d is the interatomic distance along the Si $\langle 1\,0\,0\rangle$ direction (5.43 Å). The summed energy transfers $Q(\vec{\rho})$ are given by

$$Q(\vec{\rho}) = Q(\vec{b}_1) + Q(\vec{b}_3) + Q(\vec{b}_3) + Q(\vec{b}_4), \tag{13}$$

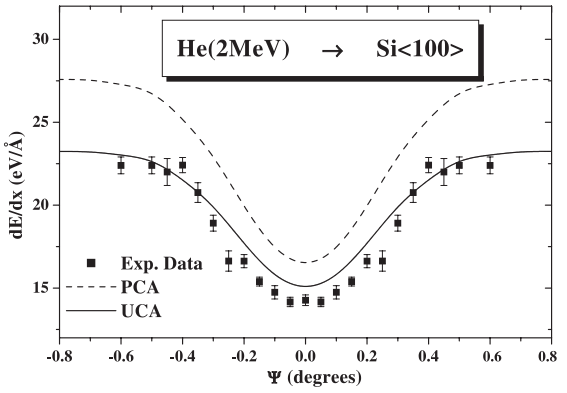

Fig. 4. Comparison of PCA and UCA calculations with experimental data (squares) on the electronic energy loss of 500 keV/u He ions channeling in Si as a function of the tilt angle Ψ of the beam relative to the $\langle 1\,0\,0\rangle$ crystal axis.

where $\vec{b}_1$, $\vec{b}_2$, $\vec{b}_3$ and $\vec{b}_4$ are the impact parameters relative to the four rows of Si atoms equidistant from the center of the $\langle 1\,0\,0\rangle$ channel.

The evaluation of the integrals in Eq. (12) requires the knowledge of the ion flux across the channel as a functions of the incidence angle Ψ. The ion flux can be obtained by solving numerically the equations of motion for an ensemble of ions impinging on the channel with entrance angle Ψ under the influence of a continuum potential. This potential is generated by adding the contributions of the four strings of atoms that form the Si $\langle 1\,0\,0\rangle$ channel.

The dashed line in Fig. 4 corresponds to the evaluation of Eq. (12) with $Q(b)$ obtained by the PCA model. Our calculations account for the energy loss due to two mechanisms: (i) Si ionization/excitation due to screened and pure Coulombic interaction with He^+ and He^{2+} projectiles ($Q^+_{ion}(b)$) and ($Q^{2+}_{ion}(b)$), respectively, and (ii) He^+ ionization, since the projectile electron can be removed due to the screened Coulomb interaction with the Si atoms ($Q_{loss}(b)$). Neglecting electron capture of an Si electron into an unoccupied He^+ state the total energy loss reads

$$Q(b) = f_1((Q^+_{loss}(b)) + (Q^+_{ion}(b))) + f_2((Q^{++}_{ion}(b))), \tag{14}$$

where f_n is the charge fraction of the He^{n+} ion inside the channel [41]. The energy loss for the He^+ beam fraction is shown in Fig. (3). The same target parameters were used to calculate the energy loss $Q^{2+}_{ion}(b)$ corresponding to the He^{2+} fraction.

As it can be observed, the PCA calculations can reproduce the width of the experimental energy loss dip. Nevertheless, the absolute values of the energy loss are significantly overestimated. This arises from the fact that first order calculations (on which PCA is based) are known to overestimate the projectile ionization probabilities and also $Q^+_{loss}(b)$ [45], since these calculations are not unitary. They do not take in account that each electronic transition gives rise to an increased final-state population and a corresponding reduction of the initial state population. It is clear that the ionization probability cannot increase indefinitely with the strength of the perturbation (the so-called saturation effect). Since these ionization processes come mostly from small impact parameters, we have to introduce, as in [28], a scaling parameter in the function h that enforces unitarity in accordance with the Bloch model. The results of these unitary convolution-approximation (UCA) calculations are displayed as a solid line in Fig. 4.

As can be seen, the UCA model yields an excellent agreement with the experimental data for the shape as well as for the absolute values of the energy loss. However, it is pointed out that there are some energy-loss processes which are not included in the UCA model. The all-over effect of these processes (influence of the band structure and dielectronic processes, capture and other higher order effects) seems to cancel, at least partially.

4. Conclusions

In this work we have described a simple model for the electronic energy loss as a function of the impact parameter for screened projectiles at high velocities. The results have been compared to full first-order calculations for the same projectile screening potential and target parameters and they were used to obtain the angular dependence of the electronic energy loss under channeling conditions (He on Si $\langle 1\,0\,0\rangle$). The comparison with full SCA calculations shows an excellent agreement. For fully screened projectiles (neutral atoms), however, special attention has to be paid to reach convergence with respect to the number of partial waves in SCA calculations. For these projectiles the SCA convergence problem is much more severe than for Coulombic ones, where the dipole term alone determines the energy loss at large impact parameters. Thus, the present PCA model does not only help to save orders of magnitude of computing time, but it also avoids convergence problems for screened projectiles.

The comparison of the PCA model with experimental channeling data reveals that the interpretation of channeling experiments with first order calculations should be made with some care. In fact, the energy-loss contributions due to

electron-loss processes (Si + He^+) are barely described in a first-order approach. Contrary, first-order calculations can be used to describe the weaker Si ionization/excitation processes by light ions at 500 keV/u reasonable well (here we find nearly no differences between PCA and UCA results). Hence, a unitary method of calculating the energy loss, such as the UCA model [28], or other non-perturbative calculations should be adopted for electron-loss process. At higher projectile velocities, however, it is expect that a first-order approach (through the PCA-screening method) for the electron-loss process will work better.

Acknowledgements

This work was partially supported by Conselho Nacional de Desenvolvimento Científico e Tecnológico (CNPq) and by the Alexander-von-Humboldt foundation.

Appendix A

For the single-zeta screened potential is the function g_{screen} reads

$$g_{\text{screen}}(b) = f_1^2 + f_2^2,$$

with $f_1(b)$ and $f_2(b)$ being

$$\begin{aligned} f_1(b) = n_p/Z_p \Bigg(& \frac{(\alpha b)^2}{2} K_0\left(\sqrt{(\omega b/v_p)^2 + (\alpha b)^2}\right) \\ & + \sqrt{(\omega b/v_p)^2 + (\alpha b)^2} K_1\left(\sqrt{(\omega b/v_p)^2 + (\alpha b)^2}\right)\Bigg) \\ & + (1 - n_p/Z_p)\omega b/v_p K_1(\omega b/v_p), \end{aligned}$$

$$\begin{aligned} f_2(b) = n_p/Z_p \Bigg(& \frac{(\alpha b)^2}{2} K_1\left(\sqrt{(\omega b/v_p)^2 + (\alpha b)^2}\right) \Bigg/ \sqrt{(\omega b/v_p)^2 + (\alpha b)^2} \\ & + (\omega b/v_p) K_0\left(\sqrt{(\omega b/v_p)^2 + (\alpha b)^2}\right)\Bigg) \\ & + (1 - n_p/Z_p)\omega b/v_p K_0(\omega b/v_p). \end{aligned}$$

and for the general screened potential we have

$$g_{\text{screen}}(b) = f_1^2 + f_2^2$$

with

$$\begin{aligned} f_1(b) = n_p/Z_p \sum_i \Bigg(& a_i K_1\left(\sqrt{(\omega b/v_p)^2 + (c_i b)^2}\right) \\ & \times \sqrt{(\omega b/v_p)^2 + (c_i b)^2} \\ & + b^2 b_i c_i K_0\left(\sqrt{(\omega b/v_p)^2 + (c_i b)^2}\right)\Bigg) \\ & + (1 - n_p/Z_p)\omega b/v_p K_1(\omega b/v_p), \end{aligned}$$

$$\begin{aligned} f_2(b) = n_p/Z_p \sum_i \Bigg(& a_i \omega b/v_p K_0\left(\sqrt{(\omega b/v_p)^2 + (c_i b)^2}\right) \\ & + b^2 \omega b/v_p b_i c_i K_1\left(\sqrt{(\omega b/v_p)^2 + (c_i b)^2}\right) \\ & \Bigg/ \sqrt{(\omega b/v_p)^2 + (c_i b)^2}\Bigg) \\ & + (1 - n_p/Z_p)\omega b/v_p K_0(\omega b/v_p). \end{aligned}$$

References

[1] A. Dalgarno, G.W. Griffing, Proc. R. Soc. London Ser. A 232 (1955) 423.
[2] Y.-K. Kim, K.-T. Cheng, Phys. Rev. A 22 (1980) 61.
[3] R. Cabrera-Trujillo, S.A. Cruz, J. Oddershede, J.R. Sabin, Phys. Rev. A 55 (1997) 2864.
[4] E.J. McGuire, Phys. Rev. A 57 (1998) 2758.
[5] P. Sigmund, Phys. Rev. A 56 (1997) 3781.
[6] T.L. Ferrell, R.H. Ritchie, Phys. Rev. B 16 (1977) 115.
[7] W. Brandt, Nucl. Instr. and Meth. 194 (1982) 13.
[8] W. Brandt, M. Kitagawa, Phys. Rev. B 25 (1982) 5631.
[9] T. Kaneko, Phys. Rev. A 30 (1984) 1714.
[10] T. Kaneko, Phys. Rev. A 33 (1986) 1602.
[11] T. Kaneko, Phys. Rev. A 41 (1990) 4889.
[12] P.M. Echenique, Nucl. Instr. and Meth. B 27 (1987) 256.
[13] A. Dygo, M.A. Boshart, L.E. Seiberling, N.M. Kabachnik, Phys. Rev. A 50 (1995) 4979.
[14] A.A. Bailes III, M.A. Boshart, L.E. Seiberling, Nucl. Instr. and Meth. 136–138 (1998) 804.
[15] Albertazzi, M. Bianconi, G. Lulli, R. Nipoli, Nucl. Instr. and Meth. B 118 (1996) 128.
[16] J.H.R. dos Santos, P.L. Grande, M. Behar, H. Boudinov, G. Schiwietz, Phys. Rev. B 55 (1997) 4332.
[17] Y. Xia, C. Tan, W.N. Lennard, Nucl. Instr. and Meth. 90 (1994) 41.
[18] N.M. Kabachnik, V.N. Kondratev, O.V. Chumanova, Phys. Stat. Sol B 145 (1988) 103.

[19] M. Moneta, J. Czerbniak, Nucl. Instr. and Meth. 90 (1994) 67.
[20] N.M. Kabachnik, O.V. Chumanova, Nucl. Instr. and Meth. B 93 (1994) 227.
[21] N.M. Kabachnik, Nucl. Instr. and Meth. B 115 (1996) 292.
[22] G. Schiwietz, Phys. Rev. A 42 (1990) 296.
[23] O. Oen, M. Robinson, Nucl. Instr. and Meth. 132 (1976) 647.
[24] O.B. Firsov, Zh. Eksp. Teor. Fiz. 36 (1959) 1517.
[25] O.B. Firsov, Sov. Phys. – JETP 9 (1959) 1076.
[26] J. Lindhard, A. Winther, K. Dan. Vidensk. Selsk. Mat. Fys. Medd. 34 (4) (1964).
[27] P.L. Grande, G. Schiwietz, Phys. Rev. A 58 (1998) 3796.
[28] G. Schiwietz, P.L. Grande, Nucl. Instr. and Meth. B 153 (1999) 1.
[29] F. Herman, S. Skillman, Atomic Structure Calculations, Prentice-Hall, Englewood Cliffs, New Jersey, 1963.
[30] E.C. Montenegro, W.E. Meyerhof, J.H. McGuire, Adv. At. Mol. Opt. Phys. 34 (1994) 249.
[31] N. Stolterfoht, Nucl. Instr. and Meth. B 53 (1991) 477.
[32] D.R. Bates, G.W. Griffing, Proc. Phys. Soc. A 68 (1955) 90.
[33] M.G. Calkin, P.J. Nicholson, Rev. Mod. Phys. 39 (1967) 361.
[34] C.O. Reinhold, J. Burgdoerfer, J. Phys. B: At. Mol. Opt. Phys. 26 (1993) 3101.
[35] J.D Jackson, Classical Electrodynamics, Wiley, 1975, Chapter 13.
[36] H.A. Bethe, R.W. Jackiw, Intermediate Quantum Mechanics, second ed., Benjamin, 1968.
[37] V.A. Khodyrev, E.I. Sirotinin, Phys. Stat. Sol B 116 (1983) 659.
[38] M. Inokuti, Rev. Mod. Phys. 43 (1971) 297.
[39] H. Bichsel, Rev. Mod. Phys. 60 (1988) 663.
[40] G. de M. Azevedo, M. Behar, J.F. Dias, P.L. Grande, J.H.R. dos Santos, R. Stoll, C. Klatt, S. Kalbitzer, Nucl. Instr. and Meth. B 136–138 (1998) 132.
[41] R.J. Petty, G. Dearnaley, Phys. Lett. A 50 (1974) 273.
[42] G. Schiwietz, P.L. Grande, Nucl. Instr. and Meth. B 69 (1992) 10.
[43] P.L. Grande, G. Schiwietz, Phys. Rev. A 47 (1993) 1119.
[44] P.L. Grande, G. Schiwietz, Nucl. Instr. and Meth. B 132 (1997) 264.
[45] P.L. Grande, G. Schiwietz, G.M. Sigaud, E.C. Montenegro, Phys. Rev. A 54 (1996) 2983.